

Pump-noise transfer in dual-pump fiber-optic parametric amplifiers: walk-off effects

F. Yaman, Q. Lin, and Govind P. Agrawal

Institute of Optics, University of Rochester, Rochester, New York 14627

S. Radic

Department of Electrical and Computer Engineering, University of California, San Diego, La Jolla, California 92093

Received November 3, 2004

Transfer of intensity noise from pumps to signal in dual-pump fiber-optic parametric amplifiers is simulated numerically for a realistic configuration in which both pumps are amplified and filtered before they enter the fiber. The walk-off effects induced by different group velocities of pumps, signal, and idler are fully taken into account. It is found that the optical signal-to-noise ratio can be as low as 15 dB when the amplifier length is close to 0.5 km, but it can be improved by 3 dB or so by use of longer fibers. © 2005 Optical Society of America

OCIS codes: 190.4970, 190.4380, 060.2320, 060.4370, 190.4410.

Fiber-optic parametric amplifiers (FOPAs) are attractive because they not only can provide large and uniform gain but also are useful for wavelength conversion and phase conjugation.^{1–7} However, since FOPAs are based on four-wave mixing (FWM) and can respond on a femtosecond time scale, they are susceptible to noise transferred from the pumps. Indeed, recent measurement on single-pump FOPAs have indicated them to be noisier than expected, with noise figures in the range of 3.7 to 4.2 dB.^{4–6} Indeed, pump fluctuations have been identified as a major source of noise for FOPAs. The transfer of relative intensity noise (RIN) from pumps to the signal is well studied in the case of Raman amplifiers.⁸ The noise-transfer problem has also been addressed for single-pump FOPAs,^{2,9,10} although these studies ignored the walk-off effects caused by the group-velocity mismatch among the pumps, signal, and idler. In this Letter we show that such walk-off effects have a major effect on pump-noise transfer. In particular, they can improve the optical signal-to-noise ratio (SNR) of the amplified signal and that of the idler (used in wavelength converters). Moreover, we extend the analysis to the case of dual-pump FOPAs as they may be better suited for some applications. Our conclusions apply to the single-pump case as well.

Most dual-pump FOPAs use two strong pumps whose wavelengths are set 40–50 nm apart but are located almost symmetrically around the zero-dispersion wavelength of the fiber.^{3,7} A nearly uniform gain is produced in this case in the spectral region between the pumps. Pump powers required by FOPAs are quite high (>0.3 W) for realizing high gain over a relatively wide gain bandwidth. When the pump wavelengths are far apart (>40 nm), gain is mostly produced by the nondegenerate FWM process in which the signal and idler interact with both pumps simultaneously. Degenerate FWM occurs around the pump wavelengths and produces a much lower gain in this region.

The most common technique for realizing high-power pumps amplifies the output of a low-power tunable laser by use of EDFAs. An optical filter is

used to reduce the amplified spontaneous emission (ASE) noise generated by EDFAs, before the pumps enter the FOPA. The residual ASE noise causes fluctuations in the pump powers. Since the signal and idler gain depend on the pump powers exponentially, fluctuations in pump power can produce much larger fluctuations in the signal and idler power. Physically, when the signal and pumps travel with the same group velocity, they remain synchronous throughout the whole fiber. As a result, different temporal slices of the signal and idler experience different pump powers and are amplified by different amounts. However, when the group-velocity mismatch among the four waves is not negligible, the net gain at the end of the fiber will correspond to the gain expected from the average power of the two pumps. The RIN transfer is considerably reduced under such conditions.

To estimate when walk-off effects become important, we compare two time scales. The first is the coherence time τ_c of pump noise, related inversely to the bandwidth B_o of the optical filter used after the EDFAs. The second time scale is the walk-off delay τ_w between the signal and pumps:

$$\tau_w \approx \frac{1}{2} \beta_3 L |(\omega_1 - \omega_3)(\omega_2 - \omega_3)|, \quad (1)$$

where β_3 is third-order dispersion of fiber, L is its length, ω_1 and ω_2 are the pump frequencies, and ω_3 is the signal frequency. As the pumps are located almost symmetrically around the zero-dispersion frequency, so are the signal and idler. Therefore the two pumps travel at the same group velocity, and the signal and idler travel together. Hence it is enough to consider group-velocity mismatch between one of the pumps and signal only. When $\tau_w \ll \tau_c$, averaging produced by walk-off becomes negligible. However, when τ_w is comparable to or larger than τ_c , the signal can experience different pump powers along the fiber, resulting in an average over pump fluctuations.

The preceding discussion suggests that an increase in τ_w helps reduce the FOPA noise. To increase τ_w , both β_3 and L in expression (1) should be as large as possible. Historically, these two parameters are al-

ways minimized as they limit the gain bandwidth. However, recent work showed that the main factors limiting gain bandwidth are fiber imperfections related to random variations in the zero-dispersion wavelength¹¹ and (or) in the residual birefringence of the fiber.¹² From the standpoint of RIN transfer, fiber length should be optimized so that it is large enough to allow averaging of the pump noise but still small enough that it does not become a limiting factor for the gain bandwidth.

We tested the validity of these physical arguments through extensive numerical simulations and found that the RIN transfer in a FOPA is indeed reduced considerably when walk-off effects are included. In numerical simulations we used the split-step Fourier method to solve the following set of four coupled equations governing the FWM process in FOPAs¹³:

$$\frac{\partial A_k}{\partial z} + \frac{1}{v_{gk}} \frac{\partial A_k}{\partial t} + \frac{id_k}{2} \frac{\partial^2 A_k}{\partial t^2} = i\beta(\omega_k)A_k + i\gamma(|A_k|^2 + 2|A_{3-k}|^2)A_k, \quad (2)$$

$$\frac{\partial A_j}{\partial z} + \frac{1}{v_{gj}} \frac{\partial A_j}{\partial t} + \frac{id_j}{2} \frac{\partial^2 A_j}{\partial t^2} = i\beta(\omega_j)A_j + 2i\gamma(|A_1|^2 + |A_2|^2)A_j + 2i\gamma A_1 A_2 A_{7-j}^*, \quad (3)$$

where $k=1$ or 2 and $j=3$ or 4 , A_1 and A_2 represent pump fields, and A_3 and A_4 are the signal and idler fields, respectively. $\beta(\omega) = \omega n(\omega)/c$ is the propagation constant at a given frequency ω , where $n(\omega)$ is the effective index of the fiber mode. The dispersion terms that appear in Eqs. (2) and (3) are usually expressed in terms of the dispersion parameters, β_n , defined at the zero-dispersion wavelength of the fiber using $\beta(\omega) = \sum_{n=0}^4 (n!) \beta_n (\omega - \omega_0)^n$, where $\beta_n = (\partial^n \beta / \partial \omega^n)|_{\omega=\omega_0}$. Group velocity v_{gm} and its dispersion d_m at any frequency ω_m can be obtained from $\beta(\omega_m)$. The pumps are strong enough that pump depletion is ignored. The nonlinear effects produced by the pumps are in-

cluded through nonlinear parameter γ .

The pumps are assumed to be relatively noise free before they are amplified by a factor of G_p by an EDFA. The ASE added by EDFAs is assumed to have a spectral density of $S_{\text{ASE}} = n_{\text{sp}}(\hbar\omega)(G_p - 1)$ for pump at frequency ω , where n_{sp} is the population inversion factor. Pumps are assumed to be filtered using filters with a 1-nm effective bandwidth. To calculate RIN spectra, we solve Eqs. (2) and (3) repeatedly for different ASE-noise seeds and perform an ensemble average over 1000 realizations numerically. We use the following definitions for the signal RIN, the pump RIN, and RIN enhancement factor F_r :

$$\text{RIN}_s(\omega, L) = \langle P_3 \rangle^{-2} \int_{-\infty}^{\infty} \langle \delta P_3(t) \delta P_3(t + \tau) \rangle \exp(-i\omega\tau) d\tau, \quad (4)$$

$$F_r(\omega) = \text{RIN}_s(\omega, L) / \text{RIN}_p(\omega, 0), \quad (5)$$

where $P_m = |A_m|^2$, $\delta P_m = P_m - \langle P_m \rangle$, and is RIN_p defined as in Eq. (4) after changing the subscript 3 to 1.

Figure 1 shows signal RIN spectra at three signal wavelengths of 1530, 1536, and 1550 nm. The short-dashed curve shows, for comparison, the pump RIN (identical for both pumps). In all cases, a 1-km-long highly nonlinear fiber was used with parameters $\lambda_0 = 1550$ nm, $\beta_3 = 0.1$ ps³/km, $\beta_4 = 0.8 \times 10^{-4}$ ps⁴/km, and $\gamma = 4.2$ W⁻¹ km⁻¹. A lower value of γ was needed to obtain 30-dB gain, as our analysis ignores dispersion and birefringence fluctuation. A noise-free input signal is launched with 10- μ W power. Pumps are located at 1525.28 and 1575.28 nm and have 0.5 W of average power after they are amplified by 27 dB by an EDFA with $n_{\text{sp}} = 1.5$. Figure 1 shows that the signal RIN is enhanced by 15 dB at low frequencies. However, the enhancement is reduced considerably for large frequencies, and for some frequencies the signal RIN is even less than the pump RIN. This is because of the averaging of high-frequency noise by the walk-off effects. Because such effects are larger for signal wavelengths that are detuned farther from the pumps, the RIN spectrum is narrower and the RIN is reduced significantly when the signal wavelength is 1550 nm (solid curve).

Figure 2 shows the RIN enhancement factor as a function of noise frequency under the conditions shown in Fig. 1. The horizontal line at the top shows, for comparison, the expected behavior when the walk-off effects are ignored. In the no-walk-off case, the signal RIN is 35 times larger than the pump RIN for all frequencies. When walk-off effects are taken into account, RIN enhancement is reduced as frequency increases and becomes nearly zero for frequencies beyond 200 GHz or so. The inset of Fig. 2 shows the rms spectral width σ_R of the RIN spectrum as a function of signal wavelength (squares). The solid curve in this inset is obtained by assuming that $\sigma_R = C/\tau_w$, where C is a fitting parameter. The good agreement reveals that the rms width of the signal

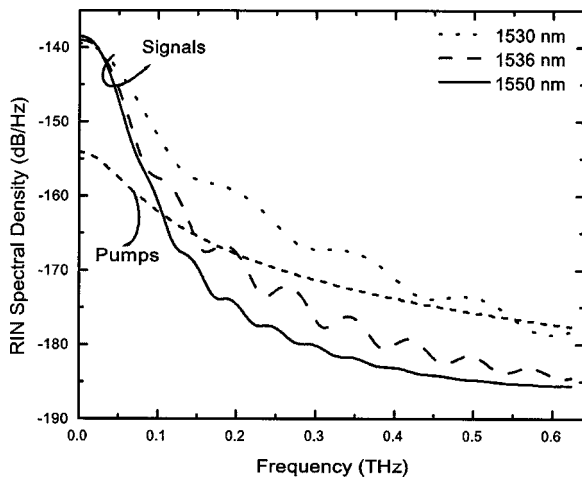


Fig. 1. RIN spectral density as a function of noise frequency at three signal wavelengths. The dashed curve shows for comparison the pump RIN spectrum.

RIN is inversely proportional to the walk-off-induced delay τ_w . Signal wavelengths that are farthest from each pump have the smallest RIN because τ_w is largest for them.

The main effect of RIN transfer is to reduce the SNR of the amplified signal. We expect the SNR to depend on the bandwidth of the optical filters used to reduce ASE noise. Figure 3 shows the optical SNR as a function of filter bandwidth for FOPA lengths of 0.5, 1, and 2 km at a fixed signal wavelength of 1555 nm. To make a meaningful comparison, the amount and the bandwidth of the FOPA gain are kept constant by keeping the product $\gamma(P_1P_2)^{1/2}L$ constant through changes in γ and by adjusting the pump wavelengths by <0.1 nm. In all cases the amplified signal is degraded severely (SNR < 18 dB) because of RIN transfer. The best SNR is realized for the longest FOPA, for which the SNR exceeds 17 dB and degrades only by <0.5 dB even if the filter bandwidth increases from 0.5 to 3 nm. This is easily understood from Fig. 3, where the width of the RIN spectrum is determined by the inverse of the walk-off parameter. When the FOPA length is relatively short and walk-off is reduced, the SNR is not only smaller but also degrades considerably with increasing filter bandwidth. The electrical SNR of the signal, on the other hand, would not be degraded as much as the optical SNR because of a much lower bandwidth of electrical filters. For a FOPA with a smaller $\beta_3 \approx 0.05$ ps²/nm, walk-off effects will be reduced by 50%.

In conclusion, we have shown that the walk-off effects can be beneficial in designing low-noise FOPAs when the primary source of noise is the ASE added by EDFAs used to amplify pumps. How much pump noise is transferred to the signal depends on the FOPA length and the bandwidth of the pump filter. Numerical simulations show that FOPA length plays a significant role, and the SNR is lower for shorter fiber lengths. From the standpoint of RIN transfer, it is better to use a longer fiber. In practice, the FOPA length should be optimized to balance the conflicting

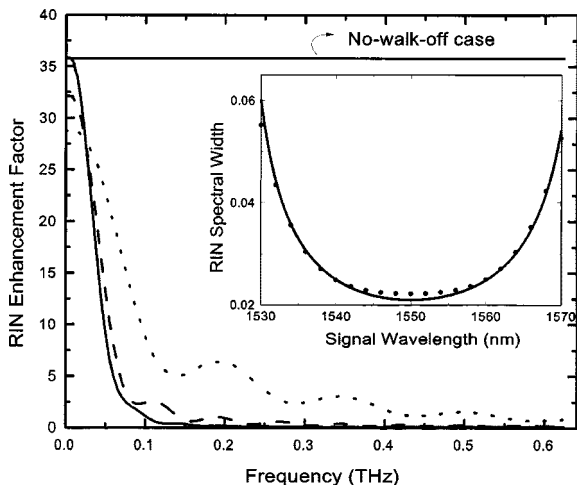


Fig. 2. F_r for the same three signal wavelengths shown in Fig. 1. The inset shows σ_R as a function of signal wavelength (filled circles) and the theoretical fit assuming that σ_R scales inversely with τ_w (solid curve).

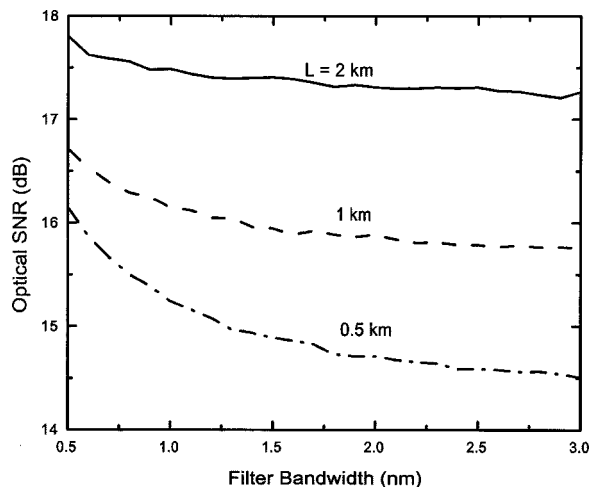


Fig. 3. Optical SNR as a function of filter bandwidth for FOPA lengths of 0.5, 1, and 2 km. The signal is at 1555 nm. All other parameters are identical to those used for Fig. 1.

requirements of a high bandwidth and a low RIN. Even though we have focused on the amplified signal, our conclusions apply to the idler as well. They indicate that the FOPA-based wavelength converters are likely to suffer from the pump-noise transfer problem and that the use of walk-off effects can help in improving their performance.

This work was supported by the U.S. National Science Foundation under grants ECS-0320816 and ECS-0334982.

References

1. J. Hansryd, P. A. Andrekson, M. Westlund, J. Li, and P. O. Hedekvist, *IEEE J. Sel. Top. Quantum Electron.* **8**, 506 (2002).
2. M. N. Islam and Ö. Boyraz, *IEEE J. Sel. Top. Quantum Electron.* **8**, 527 (2002).
3. T. Tanemura and K. Kikuchi, *IEEE Photonics Technol. Lett.* **15**, 1573 (2003).
4. P. L. Voss and P. Kumar, *Opt. Lett.* **29**, 445 (2004).
5. K. K. Y. Wong, K. Shimizu, M. E. Marhic, K. Uesaka, G. Kalogerakis, and L. G. Kazovsky, *Opt. Lett.* **28**, 692 (2003).
6. J. L. Blows and S. E. French, *Opt. Lett.* **27**, 491 (2002).
7. S. Radic, C. J. McKinstrie, R. M. Jopson, J. C. Centanni, Q. Lin, and G. P. Agrawal, *Electron. Lett.* **39**, 838 (2003).
8. C. R. S. Fludger and V. Handerek, *J. Lightwave Technol.* **19**, 1140 (2001).
9. P. Kylemark, P. O. Hedekvist, H. Sunnerud, M. Karlsson, and P. A. Andrekson, *J. Lightwave Technol.* **22**, 409 (2004).
10. G. Kalogerakis, M. E. Marhic, K. K. Y. Wong, and L. G. Kazovsky, in *Optical Fiber Communication Conference (OFC)*, Vol. 86 of OSA Trends in Optics and Photonics Series (Optical Society of America, Washington, D.C., 2003), paper CFA5.
11. F. Yaman, Q. Lin, S. Radic, and G. P. Agrawal, *IEEE Photonics Technol. Lett.* **16**, 1292 (2004).
12. F. Yaman, Q. Lin, and G. P. Agrawal, *IEEE Photonics Technol. Lett.* **16**, 431 (2004).
13. G. P. Agrawal, *Nonlinear Fiber Optics*, 3rd ed. (Academic, San Diego, Calif., 2001), Chap. 10.